International Journal of Innovative Computing, Information and Control
Volume **7**, Number **7(A)**, July **2011**

ICIC International ©2011 ISSN 1349-4198
pp. 3725–3737

LOCALIZATION OF MOBILE ROBOTS VIA AN ENHANCED PARTICLE FILTER INCORPORATING TOURNAMENT SELECTION AND NELDER-MEAD SIMPLEX SEARCH

Chen-Chien Hsu[1], Ching-Chang Wong[2], Hung-Chih Teng[2]
Nai-Jen Li[3] and Cheng-Yao Ho[2]

[1]Department of Applied Electronic Technology
National Taiwan Normal University
No. 162, He-Ping East Rd., Sec. 1, Taipei City 10610, Taiwan
jhsu@ntnu.edu.tw

[2]Department of Electrical Engineering
Tamkang University
No. 151, Ying-Chuan Rd., Tamsui, Taipei County 25137, Taiwan

[3]Department of Electrical Engineering
National Central University
No. 300, Jhongda Rd., Jhongli City, Taoyuan County 32001, Taiwan

Received February 2010; revised July 2010

Abstract. *A localization method based on an enhanced particle filter incorporating tournament selection and Nelder-Mead simplex search (NM-EPF) for autonomous mobile robots navigating in a soccer robot game field is proposed in this paper. To analyze the environment, an omnidirectional vision device is mounted on top of the robot. Through detecting the white boundary lines relative to the robot in the game field, weighting for each particle representing the robot's pose can be iteratively updated via the proposed NM-EPF algorithm. Thanks to the hybridization effect of the NM-EPF, particles converge to the actual position of the robot in a responsive way while tackling uncertainties. Simulation and experiment results have confirmed that the proposed NM-EPF has better localization performance in the soccer robot game field in comparison to the conventional particle filter.*

Keywords: Particle filter, Nelder-mead simplex search, Tournament selection, Robot localization, Soccer robot, Omnidirectional vision

1. **Introduction.** When a mobile robot moves through an environment, its actual position and orientation always differ from the position and orientation that it is commanded to hold mainly due to wheel slippage and location uncertainty [1,2]. To execute missions given to the robot, it is critically important for the robot to perceive its position in the field.

To estimate the position of the robot, sensing devices, for example, infrared sensors, ultrasonic sensors [3-5], laser range sensors [6], vision sensors, etc., are installed on the robot to explore the environment. Because of advantages in providing a rich source of environment information, vision sensors are becoming more and more popular in various applications. Many research works investigating the localization of robots mounted with cameras for sensing the environment have been conducted [7]. Because image processing is generally time-consuming, high-speed processors are required for improving computational efficiency. Thanks to the advances of embedded systems and computer hardware,

calculation burdens of image processing have been greatly relaxed to achieve the objective of real-time processing of image stream. As a result, vision-based localization for autonomous mobile robots can now be realized without substantial problems.

There are various vision-based localization techniques available for autonomous mobile robots. Among them, the application of particle filter [8,11] to robot global localization, also known as Monte Carlo localization (MCL), [7,9] is one of the most popular techniques, which approximate Bayesian Filters using random samples for posterior estimation [10]. Unfortunately, localization accuracy by conventional particle filter techniques is significantly affected by the quantity of particles [12] and environmental model [13]. To improve localization performance in terms of accuracy and convergence rate via particle filter techniques, more sensory data and particles are required during the localization process, which inevitably incurs extra computational burden. As a result, trade-off arises between the localization accuracy and computational efficiency. If the environment under consideration has many objects with similar features, the so-called kidnapped robot problem [14,15] via the particle filter methods will further deteriorate the convergence of particles in effectively estimating the position of the robot.

To improve the performance of the particle filter, an enhanced particle filter incorporating tournament selection and Nelder-Mead simplex search scheme (NM-EPF) is proposed in this paper. Focusing on the salient step of resampling of the conventional particle filters, we replace the somehow "universal-stochastic sampling" mechanism of resampling with a tournament selection scheme in the proposed enhanced particle filter. Also, a NM simplex search method, which is a high-performance local search method without using gradient information, is incorporated into the enhanced particle filter to search a fitter particle with better weight for resampling. Hybridizing the above two methods, the NM-EPF is capable of improving the accuracy in robot localization.

The rest of the paper is organized as follows. Section 2 describes the architecture of the mobile robot with omnidirectional vision. Sections 3 and 4 give preliminaries of particle filters and Nelder-Mead simplex search, respectively. Section 5 introduces the enhanced particle filter incorporating tournament selection and Nelder-Mead simplex search scheme proposed in this paper. Simulation and experimental results of the proposed NM-EPF in estimating the position of the robot in middle-sized soccer robot game field are presented in Sections 6 and 7, respectively. Conclusions are drawn in Section 8.

2. Architecture of the Mobile Robot with Omnidirectional Vision.

2.1. System architecture of the mobile robot. Figure 1 shows the system architecture of the autonomous mobile robot that we implemented to evaluate the performance of the proposed localization method, where an omnidirectional image device with a spherical mirror is mounted on top of the robot as the only device for sensing the environment. Physical appearance of the autonomous mobile robot is shown in Figure 2. Circumventing the problems of view angle limitation of planar lens cameras, the omnidirectional image device is capable of capturing omnidirectional images with a 360-degree view of the environment. The computing center, lain in the middle of the robot, is the core for data processing and planning, including analyzing images captured by the omnidirectional image device, extracting objects information, estimating robot position, deciding strategies for moving, and generating commands for navigation in the environment. The omnidirectional movement module, on the other hand, receives control commands from the computing center for decoding into PWM values to drive the motors to allow the robot to move, stop and rotate, etc.

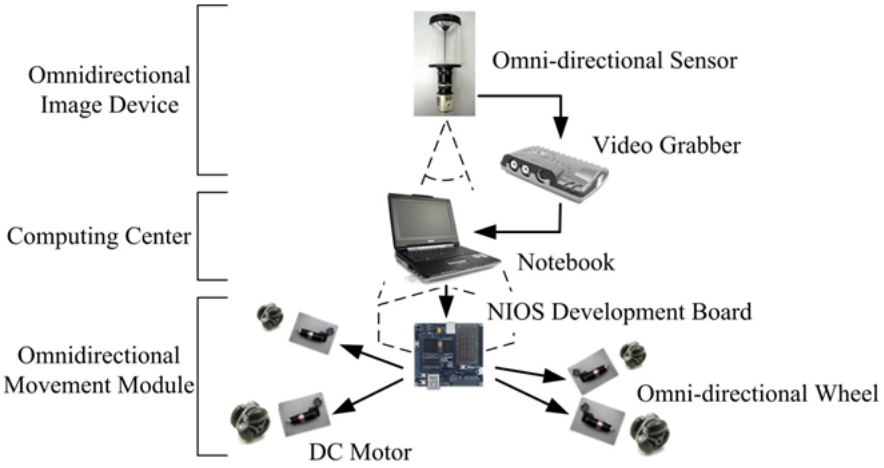

FIGURE 1. System architecture of the autonomous mobile robot

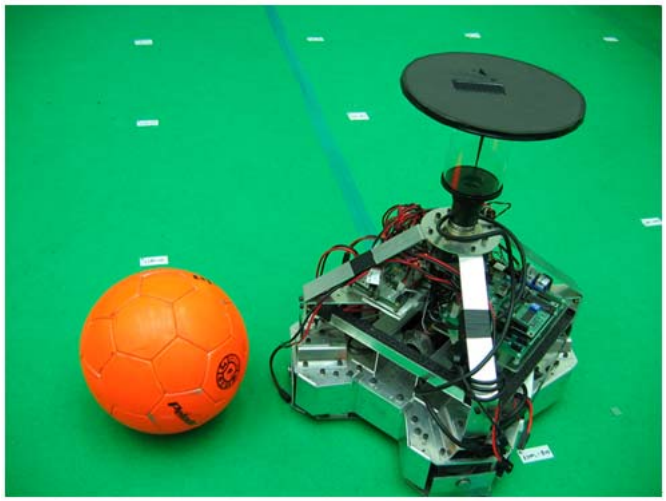

FIGURE 2. Physical appearance of the autonomous mobile robot

2.2. **Omnidirectional vision.** Compared with other range devices, vision sensors offer a rich source of object information contained in images, for example, color, size and shape, etc. It is no wonder that vision sensors are getting more and more attractive for use in autonomous robots [16]. Common planar lens cameras, however, are greatly limited by their view angle and failure to capture surrounding objects close to the robot. To solve this problem, the robot must constantly rotate the camera for grabbing images in a suitable angle. Alternatively, two or more cameras need to be set up to sense the environment. More recently, omnidirectional cameras have been used for navigation of robots. This idea has much in common with biology where the majority of insects and arthropods benefit from a wide field of view.

Figure 3 shows the formation of images by an omnidirectional image device composed of a CCD camera looking upward at a spherical mirror. The camera is mounted on top of the mobile robot with its axis placed coincident to the robot's rotation axis. Because of convex mirror reflection, the camera can grab omnidirectional images of the environment surrounding the robot with a 360-degree horizontal view. Vertical field of view depends on the curvature of the mirror.

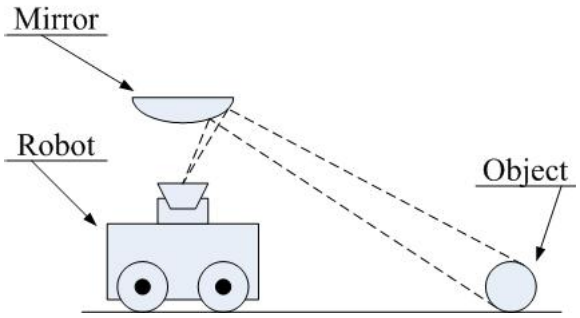

FIGURE 3. Formation of images by an omnidirectional image device mounted on a robot

3. **Preliminaries of Particle Filters.** Particle filter methods, particularly the sampling importance resampling (SIR) algorithm [17], are Monte Carlo Localization (MCL) methods that implement a recursive Bayesian filter by MC simulations. The key idea of particle filter methods is to represent the required posterior probability density function (PDF) by a set of random samples $X_k = \{x_k^1, x_k^2, \ldots, x_k^m\}$ with associated weights w_k^m to compute estimates based on these samples and weights, where m is the number of samples and k is the sample time. As the number of samples becomes sufficiently large, this MCL characterization becomes an equivalent representation to the usual functional description of the posterior PDF [18], and the SIR filter approaches the optimal Bayesian estimate.

Basically, the SIR particle filter comprises 3 steps: prediction, weight assignment and resampling [18]:

i. *Prediction*: Draw samples $X_k = \{x_k^1, x_k^2, \cdots, x_k^m\}$ from state transition probability $p(x_k \mid x_{k-1}^i, u_k)$ conditioned on x_{k-1}^i at time k for $i = 1, 2, \ldots, m$ and u_k is a control command including Gaussian noise.

$$x_k^i \sim p(x_k \mid x_{k-1}^i, u_k) \tag{1}$$

ii. *Weight assignment*: Compute the weight w_k^i of all particles for $i = 1, 2, \cdots, m$ as a probability including measurement information z_k and x_k^i of Step i.

$$w_k^i = p(z_k \mid x_k^i) \tag{2}$$

iii. *Resampling*: Draw new particles from X_k according to the normalized weight w_k^i in Step ii.

4. **The Nelder-Mead Simplex Search Method.** The NM simplex search was proposed by Nelder and Mead [19,20] as local search method for unconstrained optimization problems without using gradient information. Although the selection of starting points is sensitive in obtaining a satisfactory solution, the NM simplex search method has advantages of speedy response in solving optimization problems. As a result, we will incorporate the NM simplex scheme into the particle filter to obtain a fitter particle for subsequent resampling process.

Basically the method solves the optimization problem by continuously rescaling a n-dimensional simplex formed by $N+1$ vertex points at each iteration based on the landscape and local behavior of the function by using four basic procedures: reflection, expansion, contraction and shrinkage. Through these procedures, the simplex continuously improves itself and gets closer to the optimum X^* as iterations continue. To illustrate the operations of the method, the original NM simplex procedures are outlined below by using a two-dimensional case ($N = 2$) as an example.

i. *Initialization*: For a function of n variables, create $N+1$ vertex points to form an initial n-dimensional simplex. Evaluate the function value at each extreme point (or vertex) of the simplex.

ii. *Reflection*: Determine X_{high}, X_{sechi}, X_{low} corresponding to f_{high}, f_{sechi}, f_{low} of the highest, the second highest and the lowest objective function values, respectively. Find the center X_{cent} of the simplex excluding X_{high} (in the minimization case). A new vertex X_{refl} can be obtained by reflecting the worst point according to the following equation:

$$X_{refl} = (1+\alpha)X_{cent} - \alpha X_{high} \tag{3}$$

where α ($\alpha > 0$) is the reflection coefficient. Nelder and Mead [20] suggested that $\alpha = 1$ is chosen. If $f_{low} \leq f_{refl} \leq f_{sechi}$, accept the reflection by replacing X_{high} by X_{refl}.

iii. *Expansion*: If the reflection produces a objective function evaluation smaller than f_{low} (i.e., $f_{refl} < f_{low}$), an expansion is performed to extend the search space in the same direction for further function improvement by the following equation:

$$X_{exp} = \gamma X_{refl} + (1-\gamma)X_{cent} \tag{4}$$

where γ is the expansion coefficient ($\gamma > 1$). Nelder and Mead [20] suggested $\gamma = 2$. If $f_{exp} < f_{low}$, the expansion is accepted by replacing X_{high} with X_{exp}; otherwise, X_{refl} replaces X_{high}.

iv. *Contraction*: When X_{refl} lies between X_{high} and f_{sechi}, replaces X_{high} with X_{refl}. Contraction (outward contraction) is performed between X_{cent} and X_{high} to identify X_{cent}. If f_{refl} is larger than f_{high}, X_{refl} does not replace X_{high}, and an attempt is tried to locate X_{cont} between X_{cent} and X_{high}. The contraction vertex is calculated by the following equation:

$$X_{cont} = \beta X_{high} + (1-\beta)X_{cent} \tag{5}$$

where β is the contraction coefficient ($0 < \beta < 1$). Nelder and Mead [20] suggested $\beta = 0.5$. If $f_{cont} \leq f_{high}$, replace X_{high} with X_{cont}.

v. *Shrinkage*: If $f_{cont} > f_{high}$ in Step iv, contraction failed and shrinkage will be the next attempt. This can be done by shrinking the entire simplex (except X_{low}) by:

$$X_i \leftarrow \delta X_i + (1-\delta)X_{low} \tag{6}$$

where δ is the shrinkage coefficient ($0 < \delta < 1$). Nelder and Mead [20] suggested $\delta = 0.5$.

5. Enhanced Particle Filter Incorporating Tournament Selection and Nelder-Mead Simplex Search.

5.1. **Particle filter using tournament selection.** To reduce the degeneracy phenomenon, a resampling step is generally introduced in particle filters. The basic idea of resampling is to eliminate particles that have small weights and to concentrate on particles with large weights [18]. Among various resampling schemes, the systematic sampling scheme [21] is the most widely-adopted method, where each resampled particle $x_k^{j^*}$ is selected by criterion $C < \hat{w}_k^i$ in terms of accumulated weights. A pseudo-code description of the resampling process is given below, where $U(0,1)$ is a uniformly distributed random function:

Note that the above algorithm somehow functions like the Stochastic Universal Sampling method [22], where particles that have high weights are statistically selected many times. This leads to a loss of diversity among the particles as the resultant samples will contain many repeated points. This problem, which is known as sample impoverishment,

$[\{x_k^{j*}, w_k^{j*}\}_{j=1}^m] = \text{Resampling } [\{x_k^i,\ w_k^i\}_{i=1}^m]$
$L = \dfrac{1}{m}, \quad \hat{w}_k^i = \sum_{c=1}^{i} w_k^c, \quad C = \dfrac{1}{m}U(0,1), \quad j = 1$
For $i = 1 : m$
  While $C < \hat{w}_k^i$
    $x_k^{j*} = x_k^i, \quad w_k^{j*} = \dfrac{1}{m}$
    $C = C + L, \quad j = j + 1$
  End While
End For

is severe in the case of small process noise [18]. To address this problem, we introduce the concept of tournament selection widely used in genetic algorithm [23], where a tournament size T can be used to determine the selectivity pressure to choose particles from the current population. A pseudo-code description of the tournament selection is given below:

$[\{x_k^{l*}, w_k^{l*}\}_{l=1}^m] = \text{Tournament Selection } [\{x_k^i, w_k^i\}_{i=1}^m]$
Set tournament size T
For $l = 1 : m$
  Draw T particles randomly from $\{x_k^s, w_k^s\}_{s=1}^T$.
  Select the particle $x_k^{s'}$ with the largest weight $w_k^{s'}$
  Set $\{x_k^{l*}, w_k^{l*}\}$ as $\{x_k^{s'}, w_k^{s'}\}$
  Set $w_k^{l*} = \dfrac{1}{m}$
End For

As a result, a particle filter incorporating the tournament selection scheme to avoid the sample impoverishment problem can be obtained as follows:

i. Randomly draw particles set $X_k = \{x_k^1, x_k^2, \cdots, x_k^m\}$.
ii. Predict x_k^i using $p(x_k|x_{k-1}^i, u_k)$ for $i = 1, 2, \ldots, m$.
iii. Assign weight $w_k^i = p(z_k|x_k^i)$ for $i = 1, 2, \ldots, m$.
iv. Normalize weight $w_k^i = \dfrac{w_k^i}{\sum_{i=1}^{m} w_k^i}$ for $i = 1, 2, \ldots, m$.
v. Resample particles using tournament selection.
i. Repeat Step i to Step iv.

5.2. **Hybridization of particle filter and NM simplex search.** Although good performance in state estimation using particle filter can be obtained in general, there is still room for further improvement as far as convergence and estimation accuracy are concerned. In this section, we propose a hybrid method by incorporating a NM simple search method [24] to determine fitter particles for use in the resampling step. Figure 4 shows the flowchart of the Enhanced Particle filter incorporating a NM simplex search scheme, where the NM simplex search method is placed between the "assign weight" step and "resample" step to determine fitter particles through iterations of $N + 1$ vertex points around the particle with the highest weight. After g iterations (e.g., $g = 20$) via the NM search scheme, the fitter $N + 1$ particles can be found to replace the worst $N + 1$ particles in the population set. Because of the hybridization effect [25], where global

exploration and local exploitation are respectively achieved by the particle filter and the NM simplex search, the proposed enhanced particle filter is capable of further improving the convergence and accuracy in estimating position of the robot.

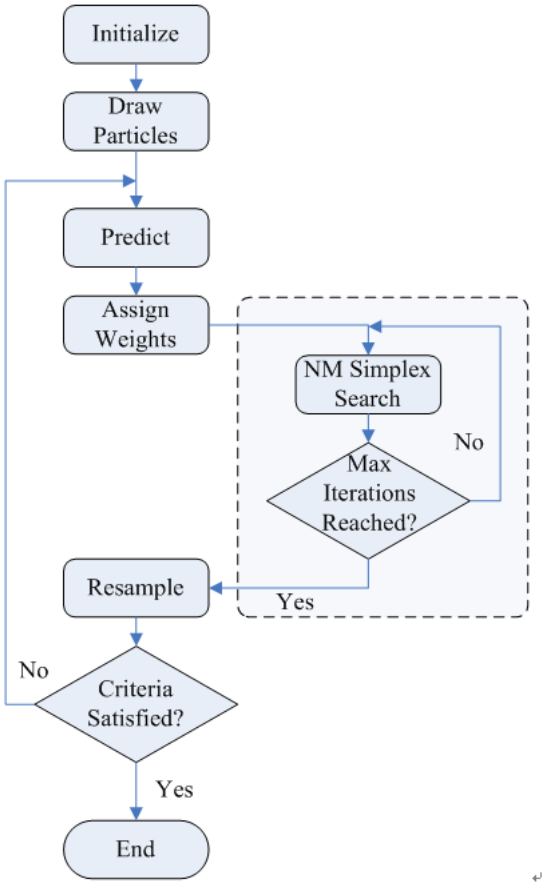

FIGURE 4. Flowchart of the enhanced particle filter incorporating a NM simplex search scheme

6. **Simulation Results.** To evaluate the performance of the proposed localization method, we adopt the F-2000 challenges of RoboCup Middle Size Robot League Rules and Regulations for 2005 to build a simulation environment of a soccer robot game field shown in Figure 5, where the center of the game filed is defined as the origin of the field coordinate system. A straight line connecting the origin and two goals forms the x axis of the field coordinate system.

To provide a faithful simulation, the sensor has a maximal sensing distance of 3 meters with a sampling interval of 4 degrees, mimicking the vision sensor during the simulation. By retrieving the surrounding distances from the white boundary lines in the game field of the simulation environment, the robot continuously explores the environment. As a result, position of the robot can be estimated via the NM-EPF by mapping the sensory information and virtual map.

Note that there exist symmetrical places in the game field, which cause serious problems during the localization process. If particles lie at these positions, they might possess a high weighting similar to the actual position of the robot, resulting in incorrect localization. Moreover, the particle with the highest weighting might "jump" from different places with strong similarity. As a result, the kidnapped robot problem occurs and the result becomes untrustworthy.

FIGURE 5. Game field of the RoboCup middle size soccer robot competition

To proceed with the simulation, the robot is instructed to navigate along a rectangle marked in dotted line in a counterclockwise direction for 140 steps (iterations) starting from the left-bottom corner in the game field. For every iteration of the particle filter, 20 extra iterations of the NM simplex search are performed to locate a fitter particle for further process by the NM-EPF. Figure 6 shows the simulation results of the localization trajectories of the robot via the NM-EPF localization scheme. Because of the symmetry of the game field, particles do not converge to the actual position of the robot until 20 iterations have been reached. As a comparison, Figure 7 shows localization errors of the mobile robot in the soccer robot game field via the NM-EPF and conventional particle filter. As demonstrated in Figure 7, the localization error is far more serious because of the kidnapped robot problem by using the conventional particle filter, which is confirmed by the mean error and standard deviation presented in Table 1. If prior knowledge of the robot's initial pose is available, initialization of the particles can be directed in a smaller area where the robot is actually located before the simulation begins. As a result of this prior knowledge during the initialization process, localization performance will be much more satisfactory as clearly demonstrated in Figure 8.

TABLE 1. Simulation results via the proposed NM-EPF localization scheme and particle filter

Methods	Error (meters)	
	Mean Error	Standard Deviation
NM-EPF	0.8813	16.7180
Particle Filter	2.6228	20.2145
NM-EPF (Initial pose known)	0.0789	9.000

7. **Practical Experiments.** To practically evaluate the performance of the proposed method, a soccer robot with omnidirectional vision and movement capability as described in Section 2 is used to navigate in an established environment identical to the FIRA RoboSot game field to conduct the experiments. Figure 9 shows the game field has a dimension of 6 meters in length and 4 meters in width. Two goals painted in yellow and blue, respectively, with a dimension of 1.2 meters in length, 0.5 meters in width, and 0.7

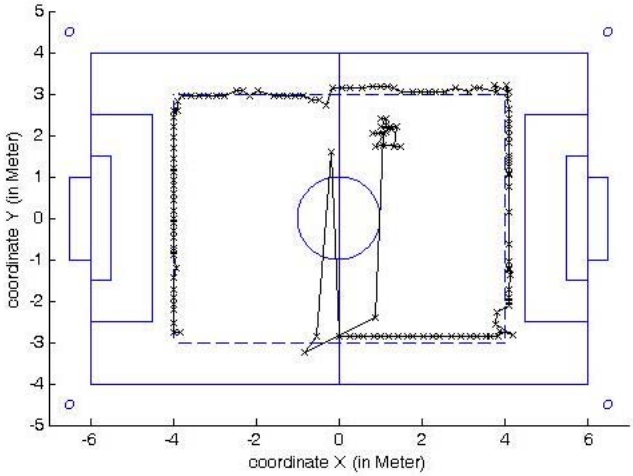

FIGURE 6. Simulation results showing localization trajectories of the robot via the NM-EPF localization scheme

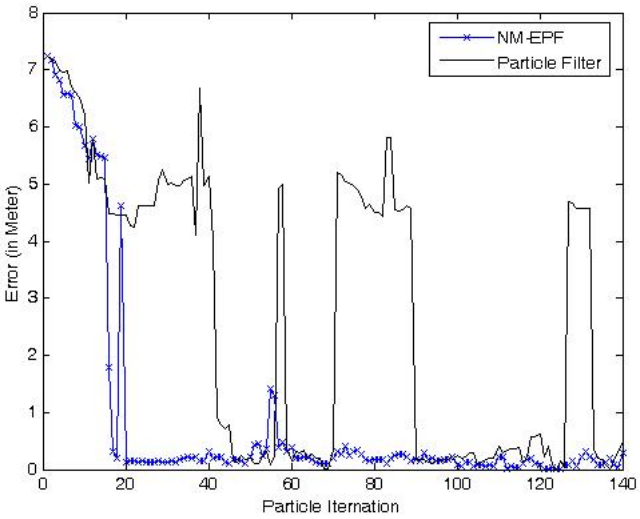

FIGURE 7. Localization errors of the mobile robot in the soccer robot game field by applying the NM-EPF and particle filter

meters in height, are positioned on two sides of the field, and four red corner cylinders are placed on four corner of the field. When expressed by Cartesian coordinate, the center of field is the origin, and the straight line connecting the origin and the blue goal forms the X axis.

Both the proposed NM-EPF and conventional particle filter are used to practically evaluate the localization performance of the robot, which is commanded to navigate along a designated path in counter-clockwise direction passing four points $(-250, 150)$, $(250, 150)$, $(250, -150)$ and $(-250, -150)$ in sequence. With the help from the omnidirectional vision and odometry feedback, both the NM-EPF and conventional particle filter manage to estimate the position of the robot to decide and adjust its movement direction, such that the navigation trajectories of the robot follows the designated path as closely as possible.

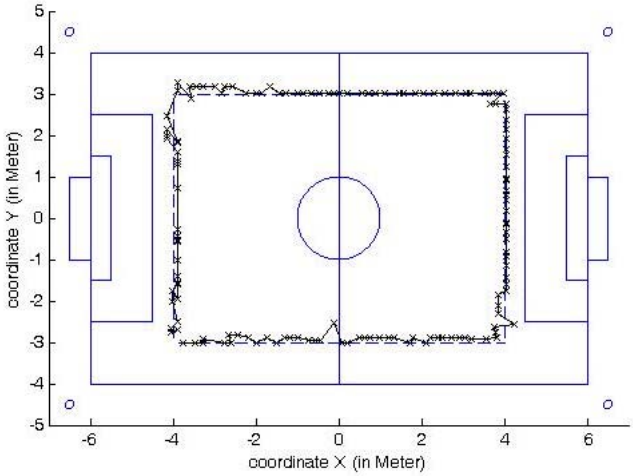

FIGURE 8. Simulation results showing localization trajectories of the robot via the NM-EPF localization scheme taking account of the prior knowledge of the robot's initial pose

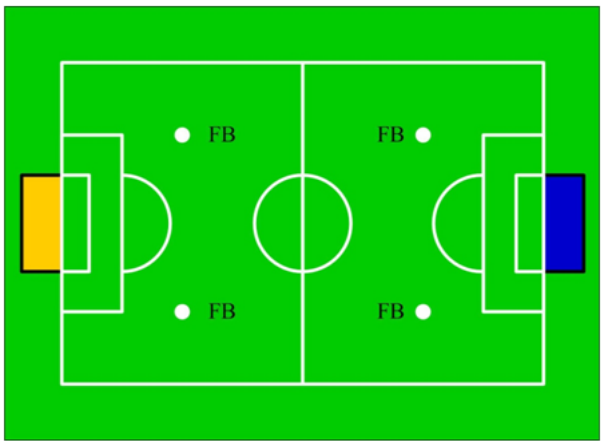

FIGURE 9. Game field of the FIRA RoboSot league

Localization results are continuously recorded for further analysis as the robot navigates. Note that there could be unexpected movement of the robot due to incorrect localization result during the initial stage when particles have not yet converged. To avoid this problem, the robot stays where it is at starting point for a short time before particles converge to the actual position after iterations of update by the localization schemes. There are 91 measurement data of the environment obtained by the omnidirectional vision each time by detecting the white lines in the game field. 500 particles are used by both of the localization schemes. 20% of the worst particles are removed and re-initialized after the resampling step to achieve better performance. Figure 10 and Figure 11 show the localization trajectories of the robot along the designated path using the NM-EPF and conventional particle filter. With a quick glance, both the NM-EPF and conventional particle filter result in similar localization performances. Nevertheless, the NM-EPF still outperforms the conventional particle filter in light of the difference

demonstrated in Table 2 in terms of mean error and standard deviation by taking average of 10 experiment results.

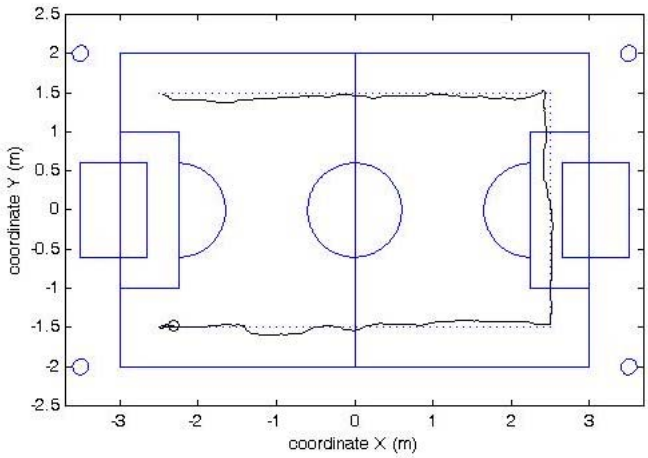

FIGURE 10. Experiment results showing localization trajectories of the robot via the NM-EPF localization scheme

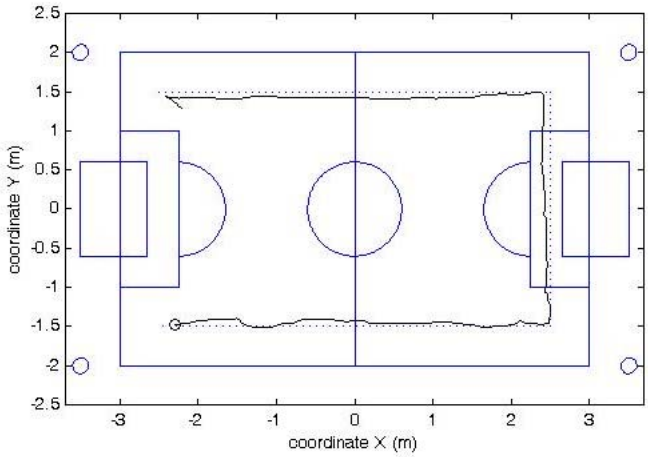

FIGURE 11. Experiment results showing localization trajectories of the robot via conventional particle filter localization scheme

8. **Conclusions.** An enhanced particle filter, NM-EPF, is proposed in this paper. Thanks to the tournament selection, the enhanced particle filter is capable of maintaining diversity among the particles, avoiding the problem of sample impoverishment. The inclusion of the NM simplex search mechanism also helps finding fitter particles with better weight for resampling. As a result, the NM-EPF converges to the correct location of the robot in a more responsive way in comparison to conventional particle filters. Simulation results have confirmed that NM-EPF is more efficient and effective to determine the actual position and orientation while alleviating the kidnapped robot problem due to symmetries

TABLE 2. Experiment results via the proposed NM-EPF and particle filter

Methods	Error (meters)		
	Mean Error	Standard Deviation	Maximum Error
NM-EPF (Initial pose known)	0.0470	0.0304	0.1200
Particle Filter (Initial pose known)	0.0628	0.0314	0.2100

in the robot soccer game field. Practical experiment results have confirmed that the NM-EPF has better localization accuracy in comparison to conventional particle filter. To be practical for use in the industry in the future, we will investigate how particle number of the proposed NM-EPF can be further reduced without affecting the localization performance so that the proposed approach can be practically applied for implementation in an embedded system for navigation purpose.

Acknowledgment. This work was partially supported by the National Science Council (NSC), Taiwan, under Grant NSC97-2221-E-032-032 and NSC94-2213-E-032-002.

REFERENCES

[1] Y.-C. Chen and Y.-T. Wang, A method for multiple-obstacle avoidance of soccer robot systems, *ICIC Express Letters*, vol.4, no.1, pp.161-168, 2010.
[2] C.-C. Wang, K.-L. Su and K.-H. Hsia, Implementation of SoPC based ZigBee wireless technology in voice-enabled robots, *ICIC Express Letters*, vol.3, no.4(A), pp.1149-1154, 2009.
[3] J. Borenstein and Y. Koren, Error eliminating rapid ultrasonic firing for mobile robot obstacle avoidance, *IEEE Transactions on Robotics and Automation*, vol.1, no.11, pp.132-138, 1995.
[4] P. Hoppenot and E. Colle, Real-time localisation of a low-cost mobile robot with poor ultrasonic data, *Control Engineering Practice*, vol.8, no.6, pp.925-934, 1998.
[5] F. Moita and U. Nunes, Multi-echo technique for feature detection and identification using simple sonar configurations, *IEEE/ASME International Conference on Advanced Intelligent Mechatronics*, vol.1, pp.389-394, 2001.
[6] H. Zhou and S. Sakane, Mobile robot localization using active sensing based on bayesian network inference, *Robotics and Autonomous Systems*, vol.4, no.55, pp.292-305, 2007.
[7] S. Thrun, W. Burgard and D. Fox, *Probabilistic Robotics (Intelligent Robotics and Autonomous Agents)*, The MIT Press, 2005.
[8] S. I. Aihara, A. Bagchi and S. Saha, On parameter estimation of stochastic volatility models from stock data using particle filter-application to AEX index, *International Journal of Innovative Computing, Information and Control*, vol.5, no.1, pp.17-28, 2009.
[9] F. Dellaert, D. Fox, W. Burgard and S. Thrun, Monte Carlo localization for mobile robots, *IEEE International Conference on Robotics and Automation*, vol.2, pp.1322-1328, 1999.
[10] S. Thrun, D. Fox, W. Burgard and F. Dellaert, Robust monte carlo localization for mobile robots, *Artificial Intelligence*, vol.128, pp.99-141, 2001.
[11] M. Tanaka, Reformation of particle filters in simultaneous localization and mapping problems, *International Journal of Innovative Computing, Information and Control*, vol.5, no.1, pp.119-128, 2009.
[12] E. Menegatti, A. Pretto, A. Scarpa and E. Pagello, Omnidirectional vision scan matching for robot localization in dynamic environments, *IEEE Transactions on Robotics*, vol.22, pp.523-535, 2006.
[13] P. Pfaff, W. Burgard and D. Fox, Robust Monte-Carlo localization using adaptive likelihood models, *Springer Tracts in Advanced Robotics*, vol.22, pp.181-194, 2006.
[14] H. Zhou and S. Sakane, Mobile robot localization using active sensing based on bayesian network inference, *Robotics and Autonomous Systems*, vol.55, pp.292-305, 2007.
[15] E. Menegatti, M. Zoccarato, E. Pagello and H. Ishiguro, Image-based monte carlo localisation with omnidirectional images, *Robotics and Autonomous Systems*, vol.48, pp.17-30, 2004.

[16] H. Tamimi, H. Andreasson, A. Treptow, T. Duckett and A. Zell, Localization of mobile robots with omnidirectional vision using particle filter and iterative SIFT, *Robotics and Autonomous Systems*, vol.54, pp.758-765, 2006.

[17] Y. C. Ho and R. C. Lee, A bayesian approach to problems in stochastic estimation and control, *IEEE Transactions on Automatic Control*, vol.9, pp.333-339, 1964.

[18] M. S. Arulampalam, S. Maskell, N. Gordon and T. Clapp, A tutorial on particle filters for online nonlinear/non-gaussian bayesian tracking, *IEEE Transactions on Signal Processing*, vol.50, pp.174-188, 2002.

[19] M. A. Luersen and R. L. Riche, Globalized Nelder-Mead method for engineering optimization, *Computers and Structures*, vol.82, pp.2251-2260, 2004.

[20] N. A. Nelder and R. Mead, A simplex method for function minimization, *Computer Journal*, vol.7, pp.308-313, 1965.

[21] G. Kitagawa, Monte carlo filter and smoother for non-Gaussian nonlinear state space models, *Journal of Computational and Graphical Statistics*, vol.1, no.5, pp.1-25, 1996.

[22] J. E. Baker, Reducing bias and inefficiency in the selection algorithm, *Proc. of the 2nd International Conference on Genetic Algorithms and their Application*, pp.14-21, 1987.

[23] B. L. Miller and D. E. Goldberg, Genetic algorithms, tournament selection, and the effects of noise, *Complex Systems*, vol.9, pp.193-212, 1995.

[24] F. Walters, L. R. Parker, S. L. Morgan and S. N. Deming, *Sequential Simplex Optimization*, CRC Press, Boca Raton, 1991.

[25] J. Lin, Y. Wu and T. S. Huang, Articulate hand motion capturing based on a Monte Carlo Nelder-Mead simplex tracker, *Proc. of the 17th International Conference on Pattern Recognition*, vol.4, pp.975-978, 2004.